

# Simultaneous trapping of low-index and high-index microparticles observed with an optical-vortex trap

K. T. Gahagan\* and G. A. Swartzlander, Jr.

Department of Physics, Worcester Polytechnic Institute, Worcester, Massachusetts 01609-2280

Received August 10, 1998; revised manuscript received November 30, 1998

We report the first observation of the simultaneous three-dimensional confinement of both a low-index particle and a high-index particle within a single-beam optical trap by using a strongly focused laser beam containing an optical vortex. Experimental and theoretical investigations of the trap stability are described. © 1999 Optical Society of America [S0740-3224(99)00904-2]  
 OCIS codes: 140.7010, 350.4990.

## 1. INTRODUCTION

Three-dimensional trapping of a transparent microparticle having a refractive index higher than the surrounding medium (a so-called high-index particle) was first demonstrated more than a decade ago with a strongly focused Gaussian beam.<sup>1</sup> Known as optical tweezers, this type of trap has found wide use in diverse fields (e.g., acoustics,<sup>2</sup> interface science,<sup>3-5</sup> biology,<sup>6-10</sup> and biophysics<sup>11-14</sup>), owing to its ability to manipulate and isolate microscopic objects in a precise and nondestructive manner. A conventional optical trap uses a highly focused TEM<sub>00</sub> Gaussian beam to attract a high-index particle into the bright focal region of the beam. In contrast, low-index particles are expelled from the beam. Several reports have shown that a doughnut-type (or vortex) beam is more efficient than a TEM<sub>00</sub> Gaussian beam at trapping high-index particles.<sup>15-17</sup> Recently we showed that a doughnut-type beam may also be used to trap low-index particles.<sup>18</sup> An additional advantage of vortex beams over Gaussian beams is that the particle is exposed to lower intensities and thus is less likely to exhibit optically induced damage. In this paper we describe a further advantage of vortex beams, namely, their ability to simultaneously trap a high-index particle and a low-index particle with a single beam.

Optical tweezers afford a sterile and noninvasive means to study particles *in situ*. Aqueous systems containing air bubbles and multiphase emulsions are examples of systems that contain both high- and low-index particles in the host solution. An ability to trap and micromanipulate these particles opens unique research and application opportunities. For example, it may be desirable to encapsulate a particle in an air bubble to inhibit interactions with the host material. Besides bubbles, low-index particles are found in water-in-oil emulsions for petroleum, food, and drug processing applications. Magneto-optic trapping of an atomic vapor by use of a vortex beam to accommodate two different atomic states may

also be possible. Indeed, the trapping of rubidium vapor in a doughnut-type beam was recently demonstrated.<sup>19</sup>

A theoretical discussion of the radiation pressure force that provides multiple stable trap sites for high- and low-index particles is given in Section 2, followed by a description of the experimental apparatus used to create such a trap in Section 3. Our observations, including a discussion of factors affecting the stability of the simultaneous trap, are described in Section 4 for an aqueous host containing high-index droplets of immersion oil and low-index hollow glass spheres (HGS's). Section 5 summarizes our findings.

## 2. THEORY

The initial scalar electric field amplitude of a monochromatic Gaussian beam containing a central vortex may be expressed in cylindrical coordinates:

$$E(\rho, \phi, z = 0) = E_0 \exp(il\phi) \tanh\left(\frac{\rho}{w_v}\right) \exp\left(-\frac{\rho^2}{w_0^2}\right) \quad (1)$$

where  $E_0$  characterizes the peak amplitude,  $w_0$  is the waist of the Gaussian envelope,  $l$  is a signed integer called the topological charge (or orbital angular-momentum quantum number), and  $w_v$  is the vortex core size. Here we assume  $|l| = 1$ . For example,  $w_v \rightarrow \infty$  for the first-order Laguerre-Gaussian beam, and  $w_v \rightarrow 0$  for an ideal point vortex.<sup>20,21</sup> The intensity profile,  $|E|^2$ , shown in Fig. 1(a), is characterized by a dark vortex core, owing to total destructive interference at the origin (where  $\phi$  is undefined). Vortices having arbitrary core sizes may be produced by computer-generated holography.<sup>22-24</sup>

When focused with a high-numerical-aperture objective, a vortex beam may trap a low-index sphere within the dark core of the vortex.<sup>18</sup> It was shown in Ref. 25 that, with the apparatus described in Section 3, the lon-



(similar to an air bubble). The buoyant force of spheres larger than  $\sim 40 \mu\text{m}$  was too large to overcome with our optical trapping forces (we used beam powers as large as 0.5 W). To isolate a concentration of smaller spheres, a volume of  $\sim 1 \text{ cm}^3$  of dry spheres was placed in the bottom of a  $10\text{-cm}^3$  graduated cylinder, and the host medium was added to fill the cylinder. The difference in buoyancy of the spheres created a size gradient in the cylinder. After approximately 1 min, liquid drawn from the bottom of the cylinder contained a majority of particles in the size range of  $R_p \sim 5$  to  $R_p \sim 15 \mu\text{m}$ . Immersion oil ( $n_p = 1.52$ ) was chosen as the high-index particle system, owing to its low absorption coefficient at the laser wavelength. We prepared an oil-in-water emulsion by combining one drop ( $\approx 0.05 \text{ ml}$ ) of immersion oil with 2 ml of the host medium. Vigorous shaking for several seconds produced an emulsion of oil droplets ranging in size from  $R'_p \sim 1$  to  $R'_p \sim 20 \mu\text{m}$ . The two dispersions were mixed and placed in a sample chamber composed of a 1-cm-diameter hole cut in a parafilm gasket ( $250 \mu\text{m}$  thick), which was sandwiched between a microscope slide and a no. 1-1/2 coverslip ( $170 \mu\text{m}$  thick), forming a sealed chamber.

#### 4. RESULTS AND DISCUSSION

In Fig. 3 we depict the simultaneous trapping of a HGS particle ( $14 \mu\text{m}$  diameter) with a smaller droplet of immersion oil ( $6 \mu\text{m}$  diameter). The first frame depicts the oil droplet, trapped a distance of  $\sim 35 \mu\text{m}$  below the coverslip (the crosshairs indicate the location of the optical axis). The larger adjacent particle is an untrapped HGS resting just below the coverslip. The image plane of the camera is adjusted to coincide with the plane  $z = z_{\text{trap}}$  located  $20 \mu\text{m}$  below the coverslip, and thus both the trapped immersion oil droplet and the untrapped HGS initially appear out of focus. The dashed circle indicates the approximate boundary of the attractive region of the low-index particle trap in the plane of the HGS. Frames 2–5 show that the HGS is pulled toward the optical axis and then down into focus to the plane  $z = z_{\text{trap}}$ . The oil droplet remains trapped below the HGS, as indicated by the remaining frames that show the two particles together, moving transversely relative to a third untrapped sphere. The typical power of the trapping beam was a few hundred milliwatts.

Interestingly, when the pair was trapped near the upper surface of the chamber, the oil droplet was more strongly trapped than the HGS, as was evident from the HGS's falling out of the trap more easily as the particles moved transversely. This result is consistent with ray-optics calculations for single-particle trapping, which predict a trapping efficiency of nearly an order of magnitude greater for the oil droplet compared with that of the HGS. The presence of the HGS is expected to scatter  $\sim 20\%$  of the light and thus only slightly reduce the oil-droplet-trapping efficiency, relative to the single-particle efficiency.

Deeper into the chamber, however, the opposite was true: the oil droplet was more weakly trapped than the HGS. In fact, with the beam focus roughly  $80 \mu\text{m}$  below the coverslip, the oil droplet fell out of the trap while the

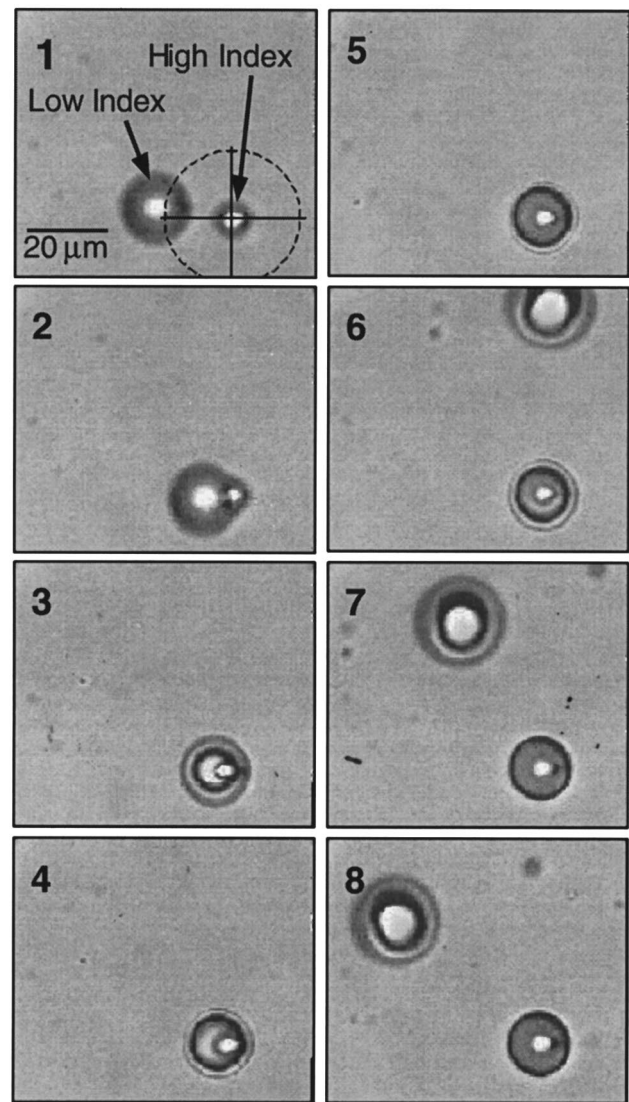


Fig. 3. Simultaneous trapping of a low-index HGS and a droplet of high-index immersion oil in water in a vortex trap. Frame 1 depicts an oil droplet ( $R'_p = 3 \mu\text{m}$ ) trapped  $\sim 35 \mu\text{m}$  below the coverslip. The crosshairs mark the location of the optical axis. The plane  $z = z_{\text{trap}}$  ( $20 \mu\text{m}$  below the coverslip) is imaged. An untrapped HGS ( $R_p = 7 \mu\text{m}$ ) rests just below the coverslip (to the left and above the oil droplet). The dashed circle represents the approximate location of the trap boundary in the plane of the HGS. In frames 2–5 the HGS moves toward the center of the trap, then down to  $z = z_{\text{trap}}$  (and into focus). In the remaining frames the two particles are transversely translated relative to a third, untrapped sphere.

HGS remained in the trap. We attribute this phenomenon to astigmatism from the glass–water interface of the coverslip.

The oil immersion objective will provide the best focusing if the host medium is index matched with the coverslip. Different refractive indices across these interfaces cause nonparaxial rays to focus closer to the coverslip than paraxial rays. This astigmatism is minimal when the beam is focused just below the coverslip, as depicted in Fig. 4(a), and hence the gradient forces on a trapped high-index particle will be optimal. Recall that a trapped

low-index particle scatters paraxial rays, leaving, as it were, the nonparaxial rays to focus and thus trap the high-index particle. If, however, the beam is focused deeply below the coverslip, the nonparaxial rays will suffer significant astigmatism, and the gradient forces will weaken. In this case, the refractive-index mismatch causes sets of nonparaxial rays to converge at points above the focal plane, as shown in Fig. 4(b), pulling the high-index particle toward the region occupied by the low-index particle. In addition, some nonparaxial rays will also scatter from the low-index particle, further weakening the trapping force, until the high-index particle falls out of the trap.

For a beam with paraxial rays focused at depth  $d_f$  below the coverslip, the shift in focusing depth,  $\Delta d$ , for a nonparaxial ray incident at angle  $\gamma_m$  is

$$\Delta d = \frac{n_0 d_f}{n_c} \left( 1 - \frac{\cos \gamma_m}{\cos \gamma_{m0}} \right) \quad (2)$$

where  $\gamma_{m0} = \sin^{-1}(n_0 \sin \gamma_m / n_c)$ ,  $n_c = 1.52$  is the refractive index of the coverslip and immersion oil, and  $n_0 = 1.33$  is the refractive index of water. For example, the trajectories of three different rays are shown in Fig. 4 for incident angles (with respect to the optical axis) of  $27^\circ$ ,  $45^\circ$ , and  $60^\circ$  and for cases in which the focal plane is positioned at depths of (a)  $d_f = 30 \mu\text{m}$  and (b)  $d_f = 100 \mu\text{m}$  below the coverslip. At the shallower depth of  $30 \mu\text{m}$ , the unscattered  $27^\circ$  and  $45^\circ$  rays pass the HGS and intercept the optical axis at points separated by only  $2 \mu\text{m}$ . A high-index particle having a size  $R_p > 2 \mu\text{m}$  may be trapped near these points (this occurrence of course depends on the beam power and the intensity distribution). Indeed, we were able to trap a  $6\text{-}\mu\text{m}$  oil droplet in our experiment. In contrast, the distance between the  $27^\circ$  and  $45^\circ$  rays is significantly larger ( $8 \mu\text{m}$ ) when the focal plane is shifted to a depth of  $d_f = 100 \mu\text{m}$  below the coverslip. From Fig. 4(b) we also see that the deviation of the  $60^\circ$  ray is so large at this depth that it scatters from the HGS.

A second factor influencing the stability of the trap is the relative size of the two particles. We found that, on average, simultaneous trapping could be achieved only when the high-index oil droplet was smaller than the HGS. For larger oil droplets, spatial overlap between the two particles prevented them from simultaneously occu-

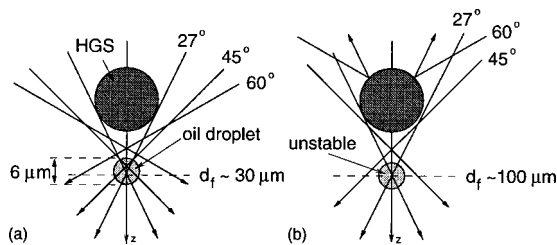


Fig. 4. Aberrations from the coverslip-water interface when the beam focus is located a distance of (a)  $d_f \sim 30 \mu\text{m}$ , and (b)  $d_f \sim 100 \mu\text{m}$  below the interface. Paraxial rays (not shown) scatter from the trapped HGS. Focused nonparaxial rays are necessary to form a high-index trap. Rays at angles as large as  $45^\circ$  contribute to the trap in (a). However, the rays are unfocused in (b), and thus the high-index particle cannot be trapped.

pying their respective trap sites. Typically, the more efficient and strongly trapped oil droplet won out in this competition. This size effect may be understood from a consideration of the spatial separation of the two trap sites. A HGS, trapped at  $z_{\text{trap}} = -2.21R_p$ , is displaced roughly one particle diameter from the beam focus. An oil droplet, on the other hand, will be trapped at a position  $z'_{\text{trap}} = 0.03R'_p$ , very nearly centered on the beam focus.

Thus overlap is expected to occur when the two particles are the same size, as is observed. When a low-index particle without a rigid boundary is used, this overlap phenomenon affords an opportunity to encapsulate a high-index particle. The two-particle trap could also be used to measure Casimir forces between particles of opposite polarizability. In addition, the existence of both a light trap and a dark trap in the same vicinity may be of interest for the trapping of cold atoms.<sup>19</sup>

For application purposes, it is of interest to know the absolute limits of particle size and refractive index that this technique affords. While there is no theoretical limit on the upper size limit of either particle, practical limits exist, since the optical force must overcome size-dependent external forces such as drag, gravitation, and buoyancy. At higher trapping powers one must also be concerned with degradation of the beam quality through heating of the objective. With our system a power of  $500 \text{ mW}$  was needed to trap the largest HGS's ( $R_p = 15 \mu\text{m}$ ). At this power polystyrene spheres of  $1\text{--}3 \mu\text{m}$  were rapidly melted in the intense beam focus. Thus we resorted to immersion oil droplets, which do not absorb  $514\text{-nm}$  light as readily. In such cases choosing a wavelength at which the particle systems are more transparent will improve performance.

Perhaps more interesting are the lower particle-size limits. In this regard, we observed oil droplets that were of the order of or smaller than the optical resolution of our imaging system ( $\sim 500 \text{ nm}$ ), trapped simultaneously with a HGS of several micrometers in diameter. We expect that this limit will be of the same order as what previous single high-index particle traps have achieved ( $\sim 25 \text{ nm}$ ), but a more well-characterized particle system is needed to be certain. The smallest low-index particles we have succeeded in trapping were of the order of  $1\text{--}2 \mu\text{m}$  in diameter (water droplets in acetophenone). Theoretically, the low-index particle must be larger than the size of the vortex core at the beam focus to prevent the particle from being pushed through the focus. However, we are not aware of any techniques capable of resolving the core size for such a strongly focused beam.

Experimentally, we have observed trapping of low-index particles with a relative refractive index ranging from  $0.75$  to  $0.87$ .<sup>25</sup> Ray-optics theory predicts that, as this value approaches unity, the location of the stable point moves away from the beam focus toward infinity in the  $-z$  direction. In this extreme the efficiency approaches zero as the percentage of the beam interacting with the particle becomes negligible. Toward the other extreme the stable position moves closer to the focus, and the width of the trap in the transverse direction narrows. The trap may then be destabilized by small perturbations to the beam profile or particle position.<sup>25</sup> For the high-

index particle the refractive index does not influence the position as strongly, but at either extreme the trapping efficiency will be reduced.<sup>16</sup>

## 5. CONCLUSIONS

We have demonstrated the simultaneous trapping of a low-index hollow glass sphere (14  $\mu\text{m}$  diameter) and a high-index immersion oil droplet (6  $\mu\text{m}$  diameter) in water by using a strongly focused optical vortex beam. For a downward propagating beam the hollow glass sphere was found to be trapped a distance of  $\sim 16 \mu\text{m}$  above the focus of the beam, while the oil droplet was believed to be trapped within 1  $\mu\text{m}$  of the focus. Once trapped, the two particles could be translated together through the sample chamber both horizontally and vertically. However, the high-index particle trap became unstable when the depth of the beam focus exceeded 80  $\mu\text{m}$ , owing to astigmatism from the glass-water interface.

## ACKNOWLEDGMENTS

This research was supported by the National Science Foundation (Young Investigator Award ECS-9457481), the Research Corporation (Cottrell Scholars Award), Spectra-Physics Lasers, Inc., and the Newport Corporation.

\*Present address, MS J585, Los Alamos National Laboratory, Los Alamos, New Mexico 87545; e-mail address, ktg@lanl.gov.

## REFERENCES

1. A. Ashkin, J. Dziedzic, J. Bjorkholm, and S. Chu, "Observation of a single-beam gradient force optical trap for dielectric particles," *Opt. Lett.* **11**, 288 (1986).
2. B. T. Unger and P. L. Marston, "Optical levitation of bubbles in water by the radiation pressure of a laser beam: an acoustically quiet levitator," *J. Acoust. Soc. Am.* **83**, 970 (1988).
3. J. C. Crocker and D. Grier, "Microscopic measurement of the pair interaction potential of charge-stabilized colloid," *Phys. Rev. Lett.* **73**, 352 (1994).
4. G. Roll, T. Kaiser, and G. Schweiger, "Optical trap sedimentation cell—A new technique for the sizing of microparticles," *J. Aerosol Sci.* **27**, 105 (1996).
5. M. Lankers, E. E. M. Khaled, J. Popp, G. Rössling, H. Stahl, and W. Kiefer, "Determination of size changes of optically trapped gas bubbles by elastic light backscattering," *Appl. Opt.* **36**, 1638 (1997).
6. W. H. Wright, G. Sonek, Y. Tadir, and M. W. Berns, "Laser trapping in cell biology," *IEEE J. Quantum Electron.* **26**, 2148 (1990).
7. A. Ashkin, J. M. Dziedzic, and T. Yamane, "Optical trapping and manipulation of single cells using infrared laser beams," *Nature (London)* **330**, 769 (1987).
8. F. Hoffmann, "Laser microbeams for the manipulation of plant cells and subcellular structures," *Plant Sci.* **113**, 1 (1996).
9. C. S. Buer, K. T. Gahagan, G. A. Swartzlander, Jr., and P. Weathers, "Threshold of power for the manipulation of *Ar<sup>+</sup>* laser beam," in *1996 Conference on In Vitro Cellular and Developmental Biology* (Society of In Vitro Biology, Landover, Md., 1996), p. 82A.
10. C. S. Buer, K. T. Gahagan, G. A. Swartzlander, Jr., and P. Weathers, "Insertion of microscopic objects through plant cell walls using laser microsurgery," *Biotechnol. Bioeng.* **60**, 348 (1998).
11. Y. Tadir, W. H. Wright, and O. Vafa, T. Ord, R. H. Asch, and M. W. Berns, "Micromanipulation of sperm by a laser generated optical trap," *Fertil. Steril.* **52**, 870 (1989).
12. K. Svoboda and S. Block, "Force and velocity measured for single kinesin molecules," *Cell* **77**, 773 (1994).
13. P. J. H. Bronkhorst, G. J. Streekstra, J. Grimbergen, J. Nijh, J. J. Sixma, and G. J. Brakenhoff, "A new method to study shape recovery of red blood cells using multiple optical trapping," *Biophys. J.* **69**, 1666 (1995).
14. M. Schindler, "The cell optical displacement assay (CODA)—measurements of cytoskeletal tension in living plant cells with a laser optical trap," *Methods Cell Biol.* **49**, 71 (1995).
15. S. Sato, M. Ishigure, and H. Inaba, "Application of higher-order-mode Nd: YAG laser beam for manipulation and rotation of biological cells," in *Conference on Lasers and Electro-Optics (CLEO/U.S.)*, Vol. 10 of 1991 OSA Technical Digest Series (Optical Society of America, Washington, D.C., 1991), p. 280.
16. A. Ashkin, "Forces of a single-beam gradient trap on a dielectric sphere in the ray optics regime," *Biophys. J.* **61**, 569 (1992).
17. N. B. Simpson, L. Allen, and M. J. Padgett, "Optical tweezers with increased trapping efficiency," in *Conference on Lasers and Electro-Optics (CLEO/U.S.)*, Vol. 11 of 1997 OSA Technical Digest Series (Optical Society of America, Washington, D.C., 1997), p. 73.
18. K. T. Gahagan and G. A. Swartzlander, Jr., "Optical vortex trapping of particles," *Opt. Lett.* **21**, 827 (1996).
19. T. Kuga, Y. Torii, N. Shiokawa, and T. Hirano, "Novel optical trap of atoms with a doughnut beam," *Phys. Rev. Lett.* **78**, 4713 (1997).
20. D. Rozas, Z. Sacks, and G. A. Swartzlander, Jr., "Experimental observation of fluidlike motion of optical vortices," *Phys. Rev. Lett.* **79**, 3399 (1997).
21. D. Rozas, C. T. Law, and G. A. Swartzlander, Jr., "Propagation dynamics of optical vortices," *J. Opt. Soc. Am. B* **14**, 3054 (1997).
22. V. Y. Bazhenov, M. S. Soskin, and M. V. Vasnetsov, "Screw dislocations in light wavefronts," *J. Mod. Opt.* **39**, 985 (1992).
23. N. R. Heckenberg, R. McDuff, and C. P. Smith, "Generation of optical phase singularities by computer-generated holograms," *Opt. Lett.* **17**, 221 (1992).
24. Z. S. Sacks, D. Rozas, and G. A. Swartzlander, Jr., "Holographic formation of optical-vortex filaments," *J. Opt. Soc. Am. B* **15**, 2226 (1998).
25. K. T. Gahagan and G. A. Swartzlander, Jr., "Trapping of low-index microparticles in an optical vortex," *J. Opt. Soc. Am. B* **15**, 524 (1998).
26. H. He, N. R. Heckenberg, and H. Rubinsztein-Dunlop, "Optical particle trapping with higher-order doughnut beams produced using high efficiency computer generated holograms," *J. Mod. Opt.* **42**, 217 (1995).
27. N. B. Simpson, L. Allen, and M. J. Padgett, "Optical tweezers and optical spanners with Laguerre-Gaussian modes," *J. Mod. Opt.* **43**, 2485 (1996).
28. H. Misawa, M. Koshioka, K. Sasaki, N. Kitamura, and H. Masuhara, "Three-dimensional optical trapping and laser ablation of a single polymer latex particle in water," *J. Appl. Phys.* **70**, 3829 (1991).
29. Tween 80 is a trademark of Aldrich Chemical Company (Milwaukee, Wis.) for the non-ionic surfactant polyoxyethylene (20) sorbitan monooleate.